Journal of Photochemistry & Photobiology A: Chemistry 361 (2018) 62–66

Contents lists available at ScienceDirect

Journal of Photochemistry & Photobiology A: Chemistry

journal homepage: www.elsevier.com/locate/jphotochem

Synthesis of 9,10-distyrylanthracene derivative and its one- and two-photon induced emission in solid state

Cong Qu[a,b], Zheng Gao[a,b], Yi Chen[a,b,*]

[a] Key Laboratory of Photochemical Conversion and Optoelectronic Materials, Technical Institute of Physics and Chemistry, The Chinese Academy of Sciences, Beijing, 100190, China

[b] University of Chinese Academy of Sciences, Beijing, 100190, China

ARTICLE INFO

Keywords:
9,10-Distyrylanthracene derivative
Solid fluorescence
Up-conversion emission
Two-photon process
Synthesis

ABSTRACT

Solid fluorescence plays an important role in optoelectronic devices. In this paper, 9,10-bis(6-dimethylamino benzoxazole styryl)-anthracene (**1**) was synthesized. **1** displayed a strong emission in solid state (microcrystalline state, amorphous solid state and polymeric thin film) resulted from aggregation-induced emission mechanism, and a large absolute fluorescence quantum yield (ϕ_f = 0.65) was obtained. **1** also exhibited up-conversion emission in solid state and a strong yellow emission was observed upon excitation with 800–1064 nm, the quadratic dependence of the fluorescence on the excitation laser intensity confirmed that the up-conversion emission resulted from two-photon process.

1. Introduction

Solid fluorescence has played an important role in optoelectronic devices such as display, laser, and biomedicine [1–6]. The molecular systems which exhibit emission in solid are usually from inorganic materials or hybrid materials, and a few examples are based on organic small molecules due to aggregation-induced emission quenching. Fortunately, some molecular systems [7–9] show unique enhanced emission rather than fluorescence quenching upon aggregation in their solid states based on aggregation induced emission or aggregation induced enhanced emission, and the discoveries have promoted research on newly fluorescent materials for their potential applications [10–12].

Up-conversion emission, generating a higher energy light from a lower energy light [13], has attracted a great deal of attention for its potential wide range of applications [14–18]. Recently, up-converted lasing based on two-photon pumped mechanism is of increasing interest since it is a new approach to accomplish frequency up-conversion of coherent light without phase-matching requirements [19,20]. The early reported materials which exhibit up-conversion emission are usually from inorganic rare earth [21–23] or metal oxides semiconductors [24–26], and few are based on organic material due to the quench of emission of organic dye in solid state. Now, more and more organic materials which exhibit up-conversion emission have been reported [27–33]. As compared to inorganic materials, organic materials exhibit more efficient nonlinear optical properties through two or more photon absorption process and tunability within a quite broad spectral range. Moreover, organic materials offer easier processing, faster response time, and lower lasing threshold. The challenge is to develop ideal organic materials with strong two-photon pumped emission in solid states.

9,10-Distyrylanthracene derivatives are a class of promising and attractive aggregation induced emission molecules [34–36], they showed many potential applications including fluorescent probe, sensors, bioimaging, optical waveguide and others [37–41]. Herein, we synthesized a new 9,10-distyrylanthracene-based fluorophore **1** (Scheme 1) and studied its one- and two-photon pumped emission in solid state. It was found that **1** exhibited weak emission in solvents but strong emission in microcrystalline or amorphous solid state, with one- or two-photon excitation, a strong emission was observed.

2. Experimental

2.1. Materials and equipment

^{1}H and ^{13}C NMR spectra were recorded at 400 and 100 MHz, respectively, with TMS as an internal reference. MS spectra were recorded with TOC-MS spectrometer, respectively. UV absorption spectra and fluorescence spectra in solution were measured with an absorption spectrophotometer (Hitachi U-3010) and a fluorescence spectrophotometer (F-2500), respectively. Fluorescence quantum yields in

* Corresponding author at: Key Laboratory of Photochemical Conversion and Optoelectronic Materials, Technical Institute of Physics and Chemistry, The Chinese Academy of Sciences, Beijing, 100190, China.
E-mail address: yichen@mail.ipc.ac.cn (Y. Chen).

https://doi.org/10.1016/j.jphotochem.2018.05.013
Received 7 March 2018; Received in revised form 7 May 2018; Accepted 11 May 2018

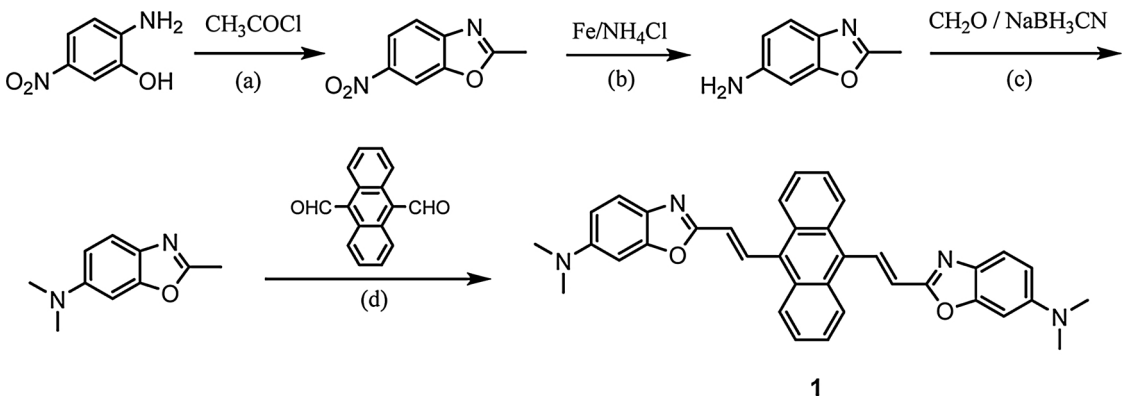

Scheme 1. Chemical structure of **1** and its synthesis.

solid state were measured with a fluorescence spectrophotometer (Edinburgh Instruments FLS-920). Solid absorption spectra were measured with UV–vis-NIR spectrophotometer (Cray 50000, Varian). All chemicals for synthesis were purchased from commercial suppliers, and solvents were purified according to standard procedures. Reaction was monitored by TLC silica gel plates (60 F-254). Column chromatography was performed on silica gel (70–230 mesh).

2.2. Experiment for two-photon pumped emission

In two-photon pumped emission experiment, a Ti-sapphire laser system (Mai Tai HP, Spectra-Physics) with a pulse width of 120 fs and a repetition rate of 82 MHz was employed as an excitation light source. The energy of excited pulse can be controlled by neutral density filters, and the beam of exciting laser was focused into the central of the cuvette with a plan-convex lens (focal length = 100 mm) under experiment. The fluorescence emitted from the sample was collected by a fiber spectrometer (SD 2000, Ocean Optics) and the direction of the detection is perpendicular to the laser transmission direction.

2.3. Molecular orbital calculations

The optimized structure of the 9,10-bis(6-dimethylamino benzoxazole styryl)-anthracene molecule was calculated at the density functional theory (DFT) level with the hybrid B3LYP functional and the 6–31 G basis set. The electron densities of the HOMO and LUMO were calculated with the Gaussian 03 package.

2.4. Synthesis of *1*

The synthetic route for **1** was outlined in Scheme 1, and the detailed procedures were presented as follows: (a) To a solution of 2-amino-5-nitrophenol (7.70 g, 50.0 mmol) and pyridine (3.96 g, 50.0 mmol) in dry xylene (150 mL) at 0 °C was added dropwise acetyl chloride (4.32 g, 55.0 mmol). The solution was stirred at ambient temperature for 2 h. To above solution was added *p*-toluenesulfonic acid (1.72 g, 10.0 mmol), the solution was refluxed till no water was discharged. After cooling to room temperature, the solution was washed with water (100 mL × 3) and a saturated solution of NaCl (50.0 mL), respectively. The organic solution was collected and dried over Na_2SO_4, after evaporation of the solvent, the crude 2-methyl-6-nitrobenzoxazole (pale solid, 8.80 g, 95% yield) was obtained for next step without purification. (b) To a solution of 2-methyl-6-nitrobenzoxazole (3.92 g, 22.0 mmol) in methanol (60.0 mL) at 70 °C was added NH_4Cl (11.77 g, 220 mmol) in H_2O (40.0 mL) and Fe (4.48 g, 80.0 mmol). The mixture solution was stirred at 70 °C for 4 h till the starting material disappeared (TLC detection). The mixture solution was cooled to ambient temperature and filtered, the solution was extracted with ethyl acetate (30.0 mL × 3). The combined organic solution was dried over Na_2SO_4, after evaporation of the solvent, the crude 2-methylbenzoxazol-6-amine (2.77 g, 85% yield) was obtained for next step reaction without purification. (c) To a solution of 2-methylbenzoxazol-6-amine (2.66 g, 18.0 mmol) in methanol (30.0 mL) was added formaldehyde (37%, 12 mL, 144 mmol) and $NaBH_3CN$ (2.27 g, 36.0 mmol). The solution was stirred at ambient temperature for 36 h till the starting material disappeared (TLC detection). The solution was poured into H_2O (30.0 mL), and the mixture solution was extracted with ethyl acetate (30.0 mL × 3). The combined organic solution was dried over Na_2SO_4, the solution is concentrated and 2-methyl-6-(*N, N*-dimethylamino) benzoxazole (2.50 g, 79% yield) is obtained by flash column chromatography (elute: petroleum ether / ethyl acetate = 10 / 1, v/v, R_f = 0.11). ^1H NMR (400 MHz, $CDCl_3$): δ = 7.46 (d, J = 8.8 Hz, 1 H), 6.78 (d, J = 2.0 Hz, 1 H), 6.74 (dd, J = 8.8 Hz, J = 2.4 Hz, 1 H), 2.97 (s, 6 H), 2.46 (s, 3 H). (d) To a solution of 2-methyl-6-(*N, N*-dimethylamino) benzoxazole (1.76 g, 10.0 mmol) and anthracene-9,10-dicarbaldehyde (1.18 g, 5.00 mmol) in dry DMF (20 mL) was added KOH (0.56 g, 10.0 mmol). The solution was stirred at 110 °C for 8 h till the starting material disappeared (TLC detection). The solid was filtered and washed with MeOH (30.0 ml), and target compound **1** (1.37 g) is obtained by flash column chromatography (elute: CH_2Cl_2). Yield: 48%. M.p. ≥ 300 °C. ^1H NMR (400 MHz, $CDCl_3$): δ (ppm) 7.91 (d, J = 16 Hz, 2 H), 7.52 (d, J = 8.8 Hz, 2 H), 7.23 (d, J = 16 Hz, 1 H), 6.73 (s, 1 H), 6.80 (d, J = 5.2 Hz, 1 H), 6.87 – 6.83 (m, 2 H), 3.05 (s, 6 H). ^{13}C NMR (100 MHz, $CDCl_3$): δ = 151.1, 150.4, 142.2, 133.8, 133.1, 129.5, 129.4, 126.2, 125.6, 124.8, 120.1, 100.3, 95.8, 41.9. TOF MS (EI) calcd for $C_{36}H_{30}N_4O_2$ (M^+): 550.2369, found: 550.2372.

3. Results and discussion

3.1. Synthesis of *1*

The synthetic details for **1** are described in the Experimental. In brief, as depicted in Scheme 1, **1** was obtained in 30% total yield by a 4-step reaction. The key intermediate *N, N*, 2-trimethylbenzoxazol-6-amine was obtained starting from 2-amino-5-nitrophenol, which condensed with acetyl chloride in xylene (98% yield), followed by reduction with NH_4Cl and Fe powder in MeOH-H_2O mixture solution (85% yield). Amino methylation was performed by the reaction of 2-methylbenzoxazol-6-amine with formaldehyde using $NaBH_3CN$ as reduction reagent to afford *N, N*, 2-trimethylbenzoxazol-6-amine in 78% yield. Treatment of *N, N*, 2-trimethylbenzoxazol-6-amine with anthracene-9,10-dicarbaldehyde in dry DMF afforded **1** in 48% yield.

3.2. Optical properties of *1* in solution

It has demonstrated [39,42] that centrosymmetric 9,10-distyrylanthracene derivatives usually possess two main absorption bands: one located at ~310 nm corresponded to the absorption of the styryl

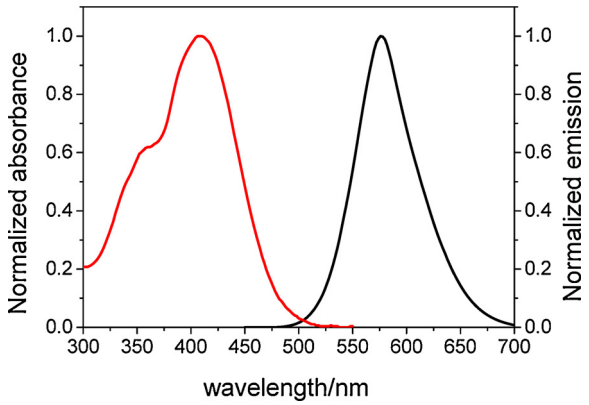

Fig. 1. Absorption and fluorescence of **1** in MeCN solution (10 μM, λ_{ex} = 420 nm).

segment, and the other at ~410 nm attributed to the π-π* transition. The optical properties of **1** in solution were conducted by measuring the absorption and the emission of **1** in dilute solutions (10 μM) in different organic solvents. In acetonitrile (MeCN), **1** showed two main absorption bands at ~360 nm and ~410 nm, respectively (Fig. 1), ~360 nm should be deduced to the absorption of benzoxazole styryl segment, a red-shift was probably due to the donor part of *N,N*-dimethylamino in benzoxazole ring, which strengthened the electron-donating ability, and ~410 nm was attributed to the π→π* transition. No significantly change in absorption spectral was obtained when **1** dissolved in other solvents such as ethanol (EtOH, λ_{max} = 410 nm) and dimethyl sulfoxide (DMSO, λ_{max} = 414 nm). A little solvatochromic effect suggested that the charge transfer transition in **1** is very small in ground state due to a centrosymmetric molecule with D-π-D-π-D structure.

Upon excitation the solution of **1** in MeCN solution, a orange fluorescence with the maximum emission wavelength at 585 nm was detected (Fig. 1), by using fluorescein (ϕ_f = 0.95, NaOH) as reference, a very small fluorescence quantum yield (ϕ_f = 0.07) was obtained. Similar results were obtained when MeCN was replaced by EtOH (λ_{em} = 587 nm, ϕ_f = 0.07). Further investigation found that **1** exhibited a positive solvatochromism: the emission wavelength was shifted to long wavelength with the increase of the polarity of solvents. In DMSO, the emission wavelength of **1** was red-shifted to 610 nm (ϕ_f = 0.01), the large solvatochromism suggested that a strong intramolecular charge transfer (ICT) occurred in the excited state, which was confirmed by both HOMO density and LUMO density of target compound **1** calcuated at the density functional theory (DFT) level with B3LYP/6-31G*. As shown in Fig. 2, the HOMO density of **1** is almost spread out over the whole π-system, while the LUMO density almost concentrates on the anthracene ring, which implies a strong ICT effect occurred when **1** was in excited state and resulted in a large solvatochromism.

3.3. One-photon induced emission of *1* in solid state

Fig. 3 represents the fluorescence spectra of **1** in microcrystalline. Upon excitation with 420 nm, a strong (absolute fluorescence quantum

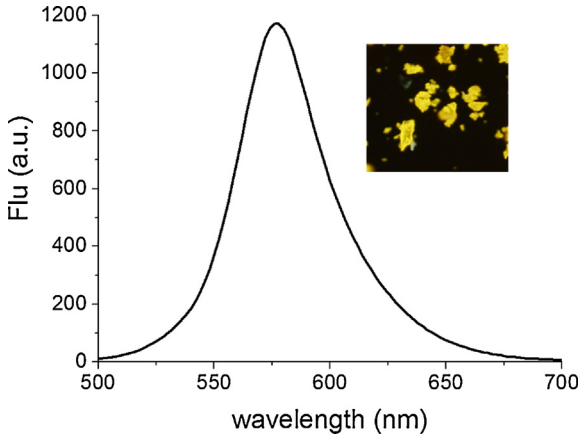

Fig. 3. Fluorescence of **1** in microcrystalline state with one-photon excitation (inset: the fluorescent imaging of **1** in microcrystalline state, λ_{ex} = 420 nm).

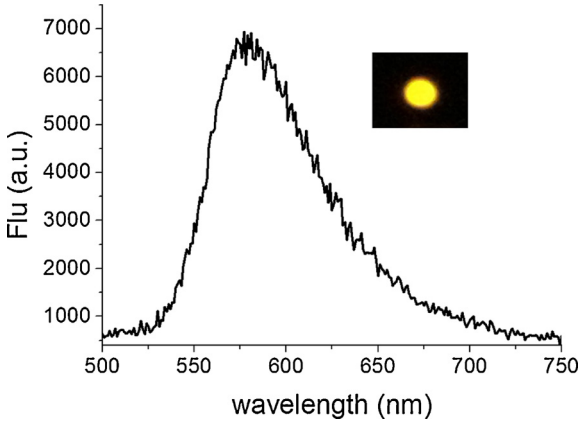

Fig. 4. Fluorescence of **1** in microcrystalline state with two-photon excitation. (inset: the fluorescent imaging of **1** in microcrystalline state, λ_{ex} = 800 nm).

yield ϕ_f = 65%), narrow (full with half maximum fwhm = 40 nm) and blue-shifted (λ_{em} = 580 nm) emission was observed (Fig. 3). As compared to solution, the emission of **1** in microcrystalline state exhibited much stronger, the enhanced fluorescence was resulted from the aggregation-enhanced emission. It has demonstrated [42] that 9,10-distyrylanthracene derivatives display a nonplanar conformation in their crystalline states due to the CH/π hydrogen bonds and exhibit strong emission as a result of the restricted torsional motion by supramolecular interaction in the crystal. As shown in Fig. 3, the intense, narrow, and blue-shifted emission of the crystal compared to that of the solutions implies that the torsional motion of **1** is unambiguously restricted by steric interaction, which leads to the closure of the nonradiative decay channel [43,44]. The distorted conformation of **1** in crystalline state limits effective conjugation and resulted in the blue-shifted emission. It is worth mentioning that a strong yellow emission was also obtained when **1** was in amorphous solid state or doped in polymeric thin films such as PMMA (polymethyl methacrylate) thin film and PS

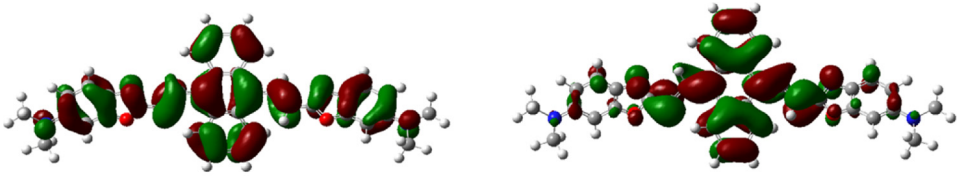

Fig. 2. Optimized molecular structure and the HOMO and LUMO electron densities of **1**.

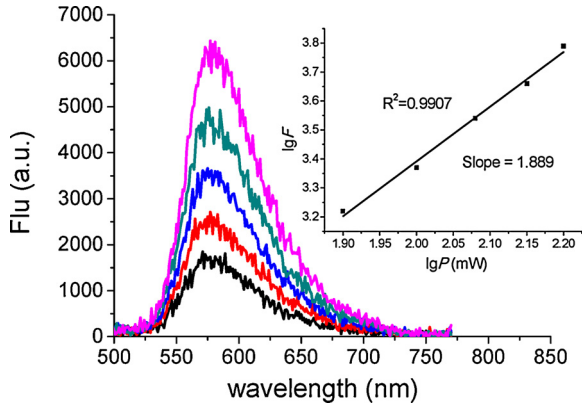

Fig. 5. Two-photon excited fluorescence changes of **1** (1.0×10^{-4} M, dichloromethane) with different excitation power (periods: 80, 100, 120, 140, 160 mW, λ_{ex} = 800 nm, inset: logarithmic plots of the dependence of two-photon induced fluorescence on pulse intensity).

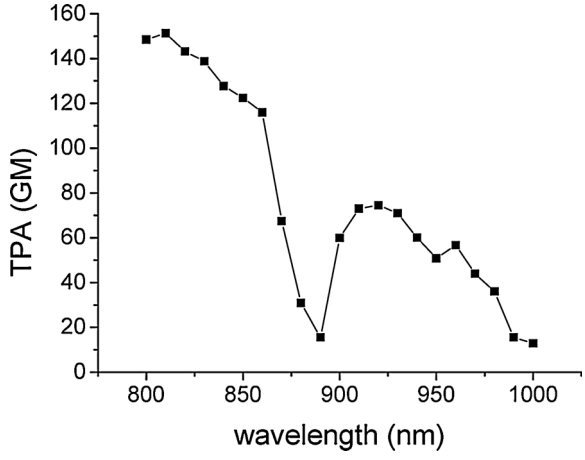

Fig. 6. Two-photon absorption spectra of **1** (1.0×10^{-4} M, dichloromethane) in 800–1000 nm region (Ti-sapphire laser, 120 fs, 82 MHz).

(polystyrene) thin film.

*3.4. Two-photon induced up-conversion emission of **1** in microcrystalline state*

Up-conversion emission of **1** in microcrystalline state were performed with Ti-sapphire femtosecond pulse laser. Upon excitation with 800 nm light, a strong yellow fluorescence with the maximum emission wavelength at 580 nm was detected (Fig. 4), which is as same as that of down-conversion emission shown in Fig. 3. Similar results were obtained upon excitation with near-infrared light source such as 980 nm and 1064 nm.

To insight into the mechanism for up-conversion emission, the fluorescence intensity changes with the change of output power was carried out. It has been known that the two-photon transition probability is proportional to the square of the excitation laser intensity [45]. Fig. 5 showed the dependence of the fluorescence of **1** in dichloromethane solution on the incident laser intensity. The least squares fit yielded a slope of 1.889 (R^2 = 0.991). The quadratic dependence of the fluorescence on the excitation laser intensity confirmed the two-photon process.

The two-photon absorption cross section (TPA cross section) was preliminary measured by two-photon fluorescence method. Since direct measurement of TPA cross section in solid state is so far technically challenging in the field of nonlinear optics, therefore, the solution of **1** was measured instead as an approximation of the property of **1** in microcrystalline state. Using fluorescein solution (pH = 11) as reference, the TPA cross sections of **1** in dichloromethane with different excitation wavelength were obtained. Fig. 6 displayed the TPA cross section of **1** in wavelegnth range of 800–1000 nm. As shown in Fig. 6, two main TPA cross sections appeared at 810 nm and 920 nm, respectively, and the largest TPA cross section (151 GM, 1 GM = 10^{-50} cm^4 $photon^{-1}$ s^{-1}) was obtained with 810 nm excitation wavelength, which is consistent with the results of similar organic compounds [46,47]. The result confirmed that **1** exhibited two-photon absorption properties which resulted in two-photon induced up-conversion fluorescence.

4. Conclusions

In summary, a new fluorophore based on 9,10-distyrylanthracene derivative with a centrosymmetric D-π-D-π-D structure has been synthesized. The fluorophore shows very weak fluorescence in solution but strong emission in microcrystalline state, the enhanced fluorescence results from aggregation-induced emission as a result of the restricted torsional motion by supramolecular interaction in crystalline state. It has demonstrated that the fluorophore exhibits nonlinear absorption property in microcrystalline state, with near-infrared excitation (800–1064 nm), a strong up-conversion emission is obtained. The quadratic dependence of the fluorescence on the excitation laser intensity confirms the two-photon process.

Acknowledgment

This work was supported by the National Natural Science Foundation of China (No 21572241).

References

[1] S.A. Swanson, G.M. Wallraff, J.P. Chen, W. Zhang, L.D. Bozano, K.R. Carter, J.R. Salem, R. Villa, J. Campbell Scott, Stable and efficient fluorescent red and green dyes for external and internal conversion of blue OLED emission, Chem. Mater. 15 (2003) 2305–2312.
[2] P. Data, A. Kurowska, S. Pluczyk, P. Zassowski, P. Pander, R. Jedrysiak, M. Czwartosz, L. Otulakowski, J. Suwinski, M. Lapkowski, A.P. Monkman, Exciplex enhancement as a tool to increase OLED device efficiency, J. Phys. Chem. C 120 (2016) 2070–2078.
[3] M. Chapran, E. Angioni, N.J. Findlay, B. Breig, V. Cherpak, P. Stakhira, T. Tuttle, D. Volyniuk, J.V. Grazulevicius, Y.A. Nastishin, O.D. Lavrentovich, P.J. Skabara, An ambipolar BODIPY derivative for a white exciplex OLED and cholesteric liquid crystal laser toward multifunctional devices, ACS Appl. Mater. Interfaces 9 (2017) 4750–4757.
[4] J.W. Sun, J.Y. Baek, K.-H. Kim, C.-K. Moon, J.-H. Lee, S.-K. Kwon, Y.-H. Kim, J.-J. Kim, Thermally activated delayed fluorescence from azasiline based intramolecular charge-transfer emitter (DTPDDA) and a highly efficient blue light emitting diode, Chem. Mater. 27 (2015) 6675–6681.
[5] H. Matsuzaki, M. Kamiya, R.J. Iwatate, D. Asanuma, T. Watanabe, Y. Urano, Novel hexosaminidase-targeting fluorescence probe for visualizing human colorectal cancer, Bioconjugate Chem. 27 (2016) 973–981.
[6] T. Fan, W. Xu, J. Yao, Z. Jiao, Y. Fu, D. Zhu, Q. He, H. Cao, J. Cheng, Naked-eye visible solid illicit drug detection at picogram level via a multiple-anchored fluorescent probe, ACS Sens. 1 (2016) 312–317.
[7] Y. Hong, J.W.Y. Lam, B.Z. Tang, Aggregation-induced emission, Chem. Soc. Rev. 40 (2011) 5361–5388.
[8] R.R. Maar, J.B. Gilroy, Aggregation-induced emission enhancement in boron difluoride complexes of 3-cyanoformazanates, J. Mater. Chem. C 4 (2016) 6478–6482.
[9] X. Fang, H. Ke, L. Li, M.-J. Lin, Structural insights into the aggregation-induced emission mechanism of naphthalene diimide solids, Dyes Pigm. 145 (2017) 469–475.
[10] X. Zhou, H. Li, Z. Chi, X. Zhang, J. Zhang, B. Xu, Y. Zhang, S. Liu, J. Xu, Piezofluorochromism and morphology of a new aggregation-induced emission compound derived from tetraphenylethylene and carbazole, New J. Chem. 36 (2012) 685–693.
[11] K. Liang, L. Dong, N. Jin, D. Chen, X. Feng, J. Shi, J. Zhi, B. Tong, Y. Dong, The synthesis of chiral triphenylpyrrole derivatives and their aggregation-induced emission enhancement, aggregation-induced circular dichroism and helical self-assembly, RSC Adv. 6 (2016) 23420–23427.
[12] G. Xie, C. Ma, X. Zhang, H. Liu, L. Yang, Y. Li, K. Wang, Y. Wei, Chitosan-based cross-linked fluorescent polymer containing aggregation-induced emission fluorogen for cell imaging, Dyes Pigm. 143 (2017) 276–283.
[13] S. Heer, K. Kompe, H.U. Gudel, M. Hasse, Highly efficient multicolour upconversion emission in transparent colloids of lanthanide-doped NaYF4 nanocrystals, Adv.

Mater. 16 (2004) 2102–2105.
[14] H.Q. Wang, M. Batentschuk, A. Osvet, L. Pinna, C.J. Brabec, Rare-earth ion doped up-conversion materials for photovoltaic applications, Adv. Mater. 23 (2011) 2675–2680.
[15] H.H. Gorris, O.S. Wolfbeis, Photon-upconverting nanoparticles for optical encoding and multiplexing of cells biomolecules, and microspheres, Angew. Chem. Int. Ed. 52 (2013) 3584–3600.
[16] G. Chen, H. Qiu, P.N. Prasad, X. Chen, Upconversion nanoparticles: design, nanochemistry, and applications in theranostics, Chem. Rev. 114 (2014) 5161–5214.
[17] M. Yu, F. Li, Z. Chen, H. Hu, C. Zhan, H. Yang, C. Huang, Laser scanning up-conversion luminescence microscopy for imaging cells labeled with rare-earth nanophosphors, Anal. Chem. 81 (2009) 930–935.
[18] N. Niu, F. He, P. Ma, S. Gai, G. Yang, F. Qu, Y. Wang, J. Xu, P. Yang, Up-conversion nanoparticle assembled mesoporous silica composites: synthesis, plasmon-enhanced luminescence, and near-infrared light triggered drug release, ACS Appl. Mater. Interfaces 6 (2014) 3250–3262.
[19] Q.D. Chen, H.H. Fang, B. Xu, J. Yang, H. Xia, F.P. Chen, W.J. Tian, H.B. Sun, Twophoton induced amplified spontaneous emission from needlelike triphenylaminecontaining derivative crystals with low threshold, Appl. Phys. Lett. 94 (2009) 201113.
[20] G.S. He, T.C. Lin, V.K.S. Hsiao, A.N. Cartwright, P.N. Prasad, L.V. Natarajan, V.P. Tondiglia, R. Jakubiak, R.A. Vaia, T.J. Bunning, Tunable two-photon pumped lasing using a holographic polymer-dispersed liquid-crystal grating as a distributed feedback element, Appl. Phys. Lett. 83 (2003) 2733–2735.
[21] J.C. Boyer, F. Vetrone, L.A. Cuccia, J.A. Capobianco, Synthesis of colloidal upconverting NaYF4 nanocrystals doped with Er3+, Yb3+ and Tm3+ Yb3+ via thermal decomposition of lanthanide trifluoroacetate precursors, J. Am. Chem. Soc. 128 (2006) 7444–7445.
[22] F. Heine, E. Heumann, T. Danger, T. Schweizer, G. Huber, B. Chai, Green upconversion continuous wave Er3+:LiYF4 laser at room temperature, Appl. Phys. Lett. 65 (1994) 383–384.
[23] Y. Li, J. Zhang, X. Zhang, Y. Luo, X. Ren, H. Zhao, X. Wang, L. Sun, C. Yan, Near infrared to visible upconversion in Er3+ and Yb3+ codoped Lu2O3 nanocrystals: enhanced red color upconversion and three-photon process in green color upconversion, J. Phys. Chem. C 113 (2009) 4413–4418.
[24] I. FortunatiI, R. Signorini, R. Bozio, J.J. Jasieniak, A. Antonello, A. Martucci, G. Della Giustina, G. Brusatin, M. Guglielmi, CdSe core − shell nanoparticles as active materials for up-converted emission, J. Phys. Chem. C 115 (2011) 3840–3846.
[25] Y. Xu, Q. Chen, C. Zhang, R. Wang, H. Wu, X. Zhang, G. Xing, W.W. Yu, X. Wang, Y. Zhang, M. Xiao, Two-photon-pumped perovskite semiconductor nanocrystal lasers, J. Am. Chem. Soc. 138 (2016) 3761–3768.
[26] Y. Wang, X. Li, X. Zhao, L. Xiao, H. Zeng, H. Sun, Nonlinear absorption and low threshold multiphoton pumped stimulated emission from all-inorganic perovskite nanocrystals, Nano Lett. 16 (2016) 448–4453.
[27] A.R. Guzman, M.R. Harpham, O. Suzer, M.M. Haley, T.G. Goodson III, Spatial control of entangled two-photon absorption with organic chromophores, J. Am. Chem. Soc. 132 (2010) 7840–7841.
[28] F. Castet, V. Rodriguez, J. Pozzo, L. Ducasse, A. Plaquet, B. Champagne, Design and characterization of molecular nonlinear optical switches, Acc. Chem. Res. 46 (2013) 2656–2665.
[29] G.S. He, T.C. Lin, V.K.S. Hsiao, A.N. Cartwright, P.N. Prasad, L.V. Natarajan, V.P. Tondiglia, R. Jakubiak, R.A. Vaia, T.J. Bunning, Tunable two-photon pumped lasing using a holographic polymer-dispersed liquid-crystal grating as a distributed feedback element, Appl. Phys. Lett. 83 (2003) 2733–2735.
[30] H.H. Fang, Q.D. Chen, J. Yang, H. Xia, B.R. Gao, J. Feng, Y.G. Ma, H.B. Sun, Two-photon pumped amplified spontaneous emission from cyano-substituted oligo(p-phenylenevinylene) crystals with aggregation-induced emission enhancement, J. Phys. Chem. C 114 (2010) 11958–11961.
[31] S. Muhammad, H.-L. Xu, R.-L. Zhong, Z.-M. Su, A.G. Al-Sehemi, A. Irfan, Quantum chemical design of nonlinear optical materials by sp2-hybridized carbon nanomaterials: issues and opportunities, J. Mater. Chem. 1 (2013) 5439–5449.
[32] S. Muhammad, A. Irfan, M. Shkir, A.R. Chaudhry, A. Kalam, S. AlFaify, A.G. Al-Sehemi, A.E. Al-Salami, I.S. Yahia, H.-L. Xu, Z.-M. Su, How does hybrid bridging core modification enhance the nonlinear optical properties in donor-π-acceptor configuration? A case study of dinitrophenol derivatives, J. Comp. Chem. 36 (2014) 118–128.
[33] S. Muhammad, A.G. Al-Sehemi, A. Irfan, H. Algarni, Y. Qiu, H. Xu, Z. Su, J. Iqbal, The substitution effect of heterocyclic rings to tune the optical and nonlinear optical properties of hybrid chalcones: a comparative study, J. Mol. Graphics Modell. 81 (2018) 25–31.
[34] R. Hu, N.L.C. Leung, B.Z. Tang, AIE macromolecules: syntheses, structures and functionalities, Chem. Soc. Rev. 43 (2014) 4494–4562.
[35] R. Balasaravanan, A. Siva, Synthesis, characterization and aggregation induced emission properties of anthracene based conjugated molecules, New J. Chem. 40 (2016) 5099–5106.
[36] Y. Wang, T. Liu, L. Bu, J. Li, C. Yang, X. Li, Y. Tao, W. Yang, Aqueous nanoaggregation-enhanced one- and two-photon fluorescence, crystalline J-aggregation-induced red shift, and amplified spontaneous emission of 9,10-bis(p-dimethylaminostyryl)anthracene, J. Phys. Chem. C 116 (2012) 15576–15583.
[37] H. Lu, B. Xu, Y. Dong, F. Chen, Y. Li, Z. Li, J. He, H. Li, W. Tian, Novel fluorescent pH sensors and a biological probe based on anthracene derivatives with aggregation-induced emission characteristics, Langmuir 26 (2010) 6838–6844.
[38] X. Zhang, X. Zhang, S. Wang, M. Liu, Y. Zhang, L. Tao, Y. Wei, Facile incorporation of aggregation-induced emission materials into mesoporous silica nanoparticles for intracellular imaging and cancer therapy, ACS Appl. Mater. Interfaces 5 (2013) 1943–1947.
[39] J. Chen, S. Ma, J. Zhang, B. Li, B. Xu, W. Tian, Low-loss optical waveguide and highly polarized emission in a uniaxially oriented molecular crystal based on 9,10-distyrylanthracene derivatives, ACS Photonics 2 (2015) 313–318.
[40] Y.-D. Lee, C.-K. Lim, A. Singh, J. Koh, J. Kim, I.C. Kwon, S. Kim, Dye/peroxalate aggregated nanoparticles with enhanced and tunable chemiluminescence for biomedical imaging of hydrogen peroxide, ACS Nano 6 (2012) 6759–6766.
[41] K.K. Ng, G. Zheng, Molecular interactions in organic nanoparticles for phototheranostic applications, Chem. Rev. 115 (2015) 11012–11042.
[42] J. He, B. Xu, F. Chen, H. Xia, K. Li, L. Ye, W. Tian, Aggregation-induced emission in the crystals of 9,10-distyrylanthracene derivatives: the essential role of restricted intramolecular torsion, J. Phys. Chem. C 113 (2009) 9892–9899.
[43] S. Kim, Q. Zheng, G.S. He, D.J. Bharali, H.E. Pudavar, A. Baev, P.N. Prasad, Aggregation-enhanced fluorescence and two-photon absorption in nanoaggregates of a 9,10-bis[4′-(4″-aminostyryl)styryl]anthracene derivative, Adv. Funct. Mater. 16 (2006) 2317–2323.
[44] W. Rettig, Charge separation in excited states of decoupled systems—TICT compounds and implications regarding the development of new laser dyes and the primary process of vision and photosynthesis, Angew. Chem. Int. Ed. Engl. 25 (1986) 971–988.
[45] S. Satapathi, L. Li, A. Kumar, H. Huo, R. Anandakathir, M. Shen, L.A. Samuelson, J. Kumar, Strong two-photon-induced fluorescence from a highly soluble polythiophene, Opt. Commun. 284 (2011) 3612–3614.
[46] Y. Wang, T. Liu, L. Bu, J. Li, C. Yang, X. Li, Y. Tao, W. Yang, Aqueous nanoaggregation-enhanced one- and two-photon fluorescence, crystalline J-aggregation-induced red shift, and amplified spontaneous emission of 9,10-bis(p-dimethylaminostyryl)anthracene, J. Phys. Chem. C 116 (2012) 15576–15583.
[47] W.J. Yang, C.H. Kim, M.-Y. Jeong, S.K. Lee, M.J. Piao, S.-J. Jeon, B.R. Cho, Synthesis and two-photon absorption properties of 9,10-bis(arylethynyl)anthracene derivatives, Chem. Mater. 16 (2004) 2783–2789.